Acta Mech 216, 281–289 (2011)
DOI 10.1007/s00707-010-0373-y

Vali Parvaneh · Mahmoud Shariati

Effect of defects and loading on prediction of Young's modulus of SWCNTs

Received: 5 May 2010 / Revised: 14 June 2010 / Published online: 3 August 2010

Abstract In this paper, the influence of various vacancy and Stone-Wales defects on the Young's modulus of single-walled carbon nanotubes is investigated via a structural model. Dispersion in experimental results is the motivation for this work. Our results show that the type of method used (loading and boundary condition) for the prediction of the Young's modulus of SWCNTs is very important for the results. The effect of different types of defects on the Young's modulus is also studied for zigzag and armchair nanotubes with various aspect ratios (length/diameter). A comparison of our results with those of experimental methods indicates that for the exact prediction of the Young's modulus of SWCNTs we need to apply the correct conditions.

1 Introduction

The discovery of carbon nanotubes by Ijimia [1] opened up a new window in nanoscience. Due to the particular mechanical and electrical features of carbon nanotubes, this kind of nanostructure has come under close scrutiny by many researchers in recent decades. A very high Young's modulus and tensile strength combined with low density give these materials excellent mechanical properties [2]. About one year after that, Ijimia [3] predicted the Young's modulus of SWCNTs at about 1 TPa. Then experimental work on the prediction of mechanical properties of SWCNTs increased. Various investigators have conducted experimental research to study the Young's modulus of carbon nanotubes. The Young's modulus can be obtained by different methods. Wong et al. [4] presented the mean experimental data as 1,280 GPa for SWCNTs by the cantilever bending method. Krishnan et al. [5] found the Young's modulus of SWCNTs to be on average 1,250 GPa for SWCNTs. They obtained their results by investigating the thermal vibrations of SWCNTs. Salvatat et al. [6] and Tombler et al. [7] reported the Young's modulus of SWCNTs of 810 and 1,200 Gpa, respectively, by the three point bending method. Yu et al. [8] reported the Young's modulus of SWCNT ropes at about 750 GPa by the tension test.

Various finite element methods have been applied for the prediction of mechanical properties of carbon nanotubes. One of them is a structural mechanics approach developed by Li and Chou [9]. In these models, interactions between carbons atoms have been modeled by beams [9–12], springs [13,14], and rods [15].

A comparison of these results with each other indicates a great amount of scattering between them. One reason for this problem can be defects. It should be noted that the quality of nanotubes used in the experiments has a significant effect on the results and the scatter of the data. Another important reason can be the type of method of experimental tests. The most commonly used instrument is atomic force microscopy (AFM), which

V. Parvaneh (✉) · M. Shariati
Department of Mechanical Engineering, Shahrood University of Technology, Daneshgah Blvd, Shahrood, Iran
E-mail: vali.parvaneh@gmail.com

V. Parvaneh
Member of the Young Researchers Club of Azad University of Mashhad, Mashhad, Iran

is used to apply loads to the nanotube in bending and tension tests. The necessity of desirable conditions for experimental tests and limitations in the instruments used are other reasons for the large scatter in experimental data. Many theoretical and numerical models have also been employed for the prediction of the Young's modulus [16–27]; however, the tension test is used by all of them. Therefore, we will not focus on modeling and simulation results, as dispersion in the results is due to their models and not the type of loading method.

Therefore, this paper investigates the effect of different vacancy and Stone-Wales defects on the Young's modulus of SWCNTs. In addition to the effect of defects, we studied the effect of different loading and boundary conditions. Here, we examine the Young's modulus of SWCNTs by four usual mechanical methods: tension, free-fixed bending, simple-simple bending and fixed-fixed bending.

The model for the carbon nanotubes is an atomistic modeling technique using ABAQUS software. This atomistic modeling technique is the molecular structural mechanics approach, which has been successfully used for the prediction of the elastic axial buckling of carbon nanotubes under compressive loads [28].

2 Application of the structural model to SWCNTs

We have proposed a structural mechanics method to model the carbon nanotubes. The detailed derivation procedure for the formulation and other features of this model can be found in our previous work [28].

The total steric potential energy due to interactions between carbon atoms can be represented by Eq. (1) [29]:

$$u_{\text{total}} = u_r + u_\theta + u_\phi + u_\omega, \tag{1}$$

where u_r, u_θ, u_ϕ, and u_ω are bond energies associated with bond stretching, angle variation or bond bending, dihedral angle torsion, and out-of-plane torsion, respectively.

In this model, Morse potentials are employed for stretching and bending potentials, and a periodic type of bond torsion is applied for torsion and out-of-plane torsion interactions (Eqs. (2)–(5)),

$$u_r = D_e \left\{ [1 - e^{-\beta(r-r_0)}]^2 - 1 \right\}, \tag{2}$$

$$u_\theta = \frac{1}{2} k_\theta (\theta - \theta_0)^2 \left[1 + k_{\text{sextic}} (\theta - \theta_0)^4 \right], \tag{3}$$

$$u_\phi = \frac{1}{2} k_\phi \left[1 + \cos(n\phi - \phi_0) \right], \tag{4}$$

$$u_\omega = \frac{1}{2} k_\omega \left[1 + \cos(n\omega - \omega_0) \right]. \tag{5}$$

As indicated in Figs. 1a and 2, a nonlinear axial spring is used for modeling of the angle variation interaction between atoms. The relationship between changes in the bond and the corresponding change in length of the spring for small displacements can be expressed simply by Eq. (7) [15],

$$\Delta\theta \approx \frac{2(\Delta R)}{r_0}, \quad r_0 = 0.142\,\text{nm}. \tag{6}$$

Therefore, we can simplify Eq. (3) to Eq. (7),

$$u_\theta = \frac{2}{r_0^2} k_\theta (R - R_0)^2 \left[1 + \frac{16}{r_0^4} k_{\text{sextic}} (R - R_0)^4 \right]. \tag{7}$$

The stretch force, the angle variation moment, the dihedral angle torque, and out-of-plane torque can be obtained from differentiations of (Eqs. (2), (4), (5), (7)) as functions of bond stretch, bond angle, dihedral angle, and out-of-plane angle variation, respectively:

$$F(r - r_0) = 2\beta D_e \left[1 - e^{-\beta(r-r_0)} \right] e^{-\beta(r-r_0)}, \tag{8}$$

$$F(R - R_0) = \frac{4}{r_0^2} k_\theta (R - R_0) \left[1 + \frac{16}{r_0^4} \left(1 + \frac{4}{r_0^2} \right) k_{\text{sextic}} (R - R_0)^4 \right], \tag{9}$$

$$T(\phi - \phi_0) = \frac{1}{2} k_\phi n \sin(n\phi - \phi_0), \tag{10}$$

$$T(\omega - \omega_0) = \frac{1}{2} k_\omega n \sin(n\omega - \omega_0). \tag{11}$$

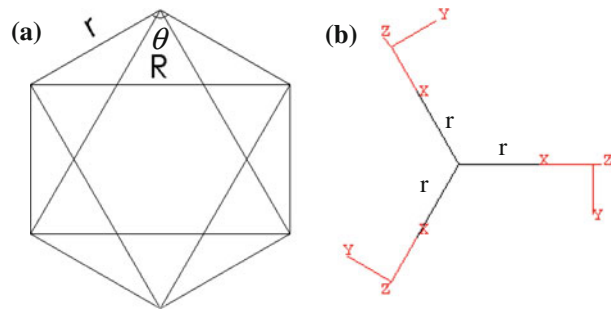

Fig. 1 **a** A hexagonal unit cell, **b** Location of local coordinates of each connector

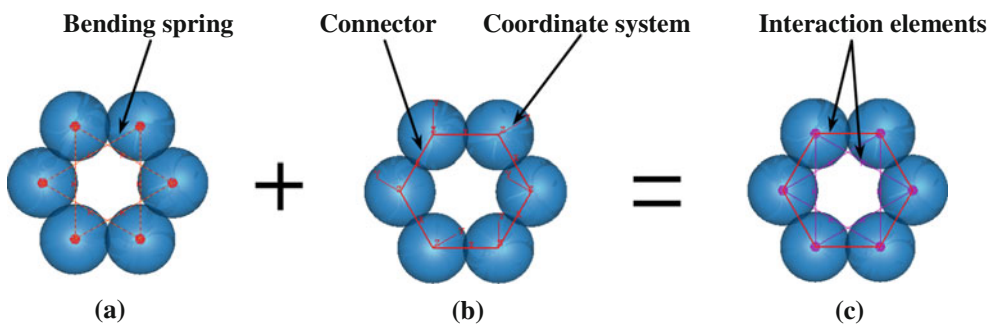

Fig. 2 Spring and connector elements corresponding to the interactions of carbon atoms. **a** The angle variation interactions, **b** the stretching and torsional interactions, **c** total interactions [28]

A nonlinear connector is considered for modeling of the stretching and torsional interactions, and a nonlinear spring for modeling of the angle variation interaction (see Fig. 2). Carbon atoms in ABAQUS are modeled by a discrete rigid sphere so that connector elements between atoms are adjoined to reference points at the center of the sphere, and a local coordinate is set at the center of each atom (see Figs. 1b and 2). This local coordinate is a combination of a Cartesian coordinate for stretching and a rotational coordinate for torsion. The X direction of these coordinates is in the connector direction, and the Z direction is vertical to the central axis of the nanotube. Because we can only use a linear spring in the CAE space of ABAQUS, by changing the linear spring command to a nonlinear spring command in the input file, and by applying the nonlinear data for $\mathrm{F}(\Delta R)$ versus ΔR using Eq. (9), we can apply the bond bending spring to the model. For applying bond stretch and torsion forces to the connectors, we can apply the nonlinear stiffness in three directions (X, Y, Z) directly. For stretching stiffness in the X direction, we can obtain the nonlinear data for $\mathrm{F}(\Delta r)$ versus Δr by Eq. (8), and for torsional stiffness in X direction, we can obtain the nonlinear data for $\mathrm{T}(\Delta\phi)$ versus $\Delta\phi$ by Eq. (10). For torsional stiffness in the Y direction, we can obtain the nonlinear data for $T(\Delta\omega)$ versus $\Delta\omega$ by Eq. (11).

Here, we take $E = 1{,}170\,\mathrm{GPa}$ and $\nu = 0.196$ for the Young's modulus and Poisson's ratio of single-walled carbon nanotubes, respectively. As shown in our previous work, we used $k_r = 800\,\mathrm{nN/nm}$, $k_\theta = 1.42\,\mathrm{nN/nm.Rad}^{-2}$, $k_\phi = k_\omega = 0.0418\,\mathrm{nN.nm}$, which are consistent with the values reported in the literature. This structural model was successfully used for predicting the mechanical properties and axial buckling behavior of single-walled carbon nanotubes. It is employed here for predicting the Young's modulus of single-walled carbon nanotubes.

3 Four methods for the prediction of the Young's modulus of perfect SWCNTs

The tension test is one of the well-known methods for the prediction of the Young's modulus of materials. To find the exact Young's modulus of a circular shell on the macroscale, we usually construct a standard segment from materials and test it instead of the circular shell. However, we cannot apply this method for materials on the nanoscale, such as carbon nanotubes. Therefore, in the tension test for a carbon nanotube, we stretch the carbon nanotubes from tow ends. Here, we fix the tow plane at the ends of the nanotube and apply a uniaxial force to the center of the tow planes (see Fig. 3a). We performed the tension test on perfect

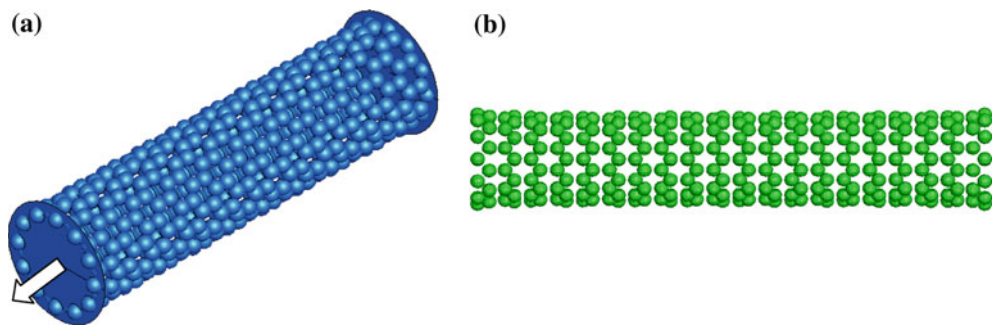

Fig. 3 Boundary and loading conditions of the structural model of SWCNTs (**a**) and deformed configuration of zigzag (12, 0) subjected to tension (**b**)

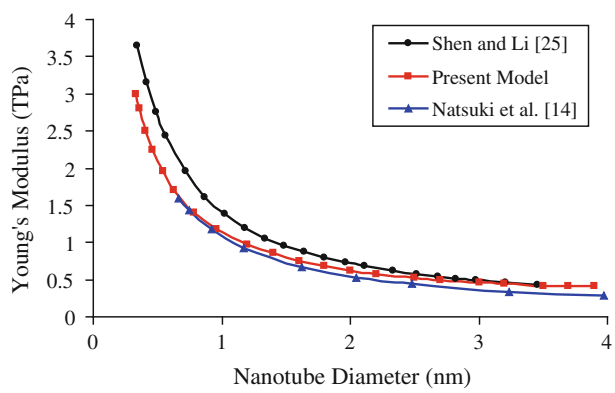

Fig. 4 Comparison of the present results to results of the molecular mechanics model [25] and the analytical structural model [14] for zigzag nanotubes

zigzag (12, 0) and armchair (7,7) SWCNTs with various aspect ratios (L/d). Figure 3b shows the deformed configuration of a perfect zigzag (12, 0) nanotube after the tension test.

To verify the above-described model, in Fig. 4, we have compared the present results to those of Shen and Li [25] and Natsuki et al. [14]. From this figure, it can be found that the present results of the zigzag model are very close to those of Shen and Li [25] for large diameters and very close to Natsuki [14] for small diameters.

We also obtained the Young's modulus by bending tests. Three types of bending tests are shown in Fig. 5. For short lengths of the nanotubes, local bending will occur (see Fig. 2b), and for longer nanotubes, global bending will occur (see Fig. 5c, d). The Young's modulus of a SWCNT from free-fixed, fixed-fixed and simple-simple bending tests is obtained from continuum mechanics, Eqs. (12–14), respectively:

$$E = \frac{FL^3}{6\delta I}, \tag{12}$$

$$E = \frac{5FL^3}{96\delta I}, \tag{13}$$

$$E = \frac{FL^3}{48\delta I}, \tag{14}$$

where L, I, F and δ are the length of the nanotube, the cross-sectional moment of inertia, the applied force and the displacement of the center of the nanotube, respectively. The effective wall thickness of SWCNTs is 0.34 nm. These three equations are obtained from continuum mechanics theories and utilized for continuum beams.

The Young's modulus is found by four mechanical methods for perfect nanotubes with different aspect ratios and is compared with each other (see Fig. 6). It is seen from Fig. 6 that the Young's modulus for both armchair and zigzag nanotubes increases with increasing aspect ratio and approaches a constant value. This increase is lacking for the tension test; however, it is present in free-fixed bending and much more so in simple-simple and fixed-fixed bending. For more accurate experimental tests, we must use sufficiently long nanotubes.

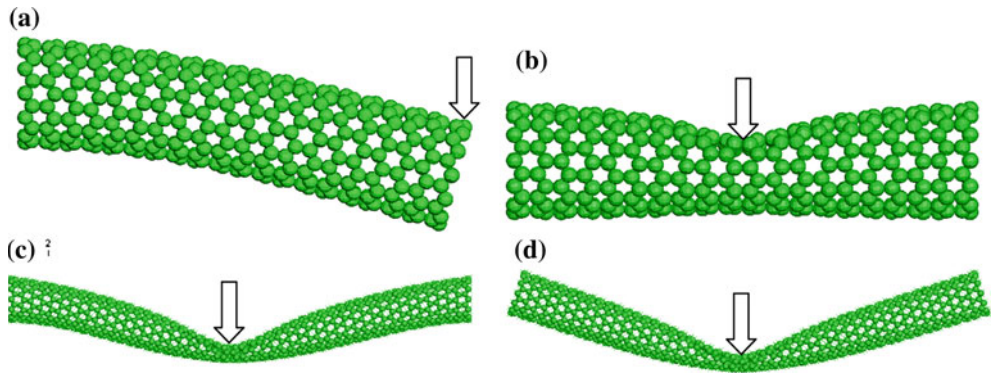

Fig. 5 Deformed shape of free-fixed zigzag (12, 0) subjected to bending (**a**), local bending of fixed-fixed zigzag (**b**), global bending of fixed-fixed zigzag (**c**), global bending of simple-simple zigzag (**d**)

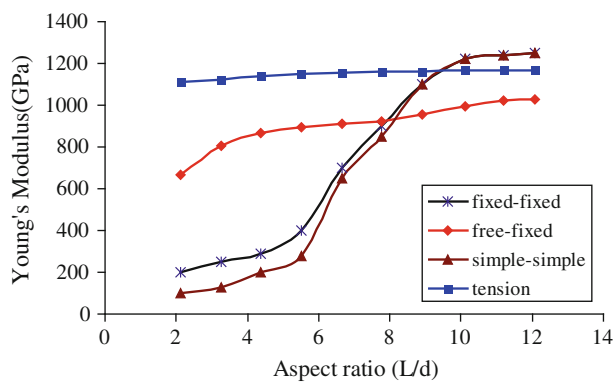

Fig. 6 Young's modulus of single-walled carbon nanotube as a function of nanotube aspect ratio

The comparison of the Young's modulus obtained by the four methods indicates that the predicted Young's modulus from the tension test results for different aspect ratios is approximately constant; the Young's modulus of each material is constant and does not depend on geometrical parameters, and hence it seems that the tension test presents the best results. However, with increasing length of the nanotube, the predicted Young's modulus by the three bending tests will increase and approach a constant value. For sufficiently long nanotubes, the minimum predicted value for the Young's modulus by these four methods is dependent on free-fixed bending, and the maximum value depends on simple-simple and fixed-fixed bending. It appears that the best method for the prediction of the Young's modulus of carbon nanotubes is the tension test because in addition to the above-noted advantage, the predicted Young's modulus by this method is moderate.

From a length of 5 nm and up, we have seen that the Young's modulus increases significantly for the fixed-fixed and simple-simple bending methods. This change is due to the variation of the mode shapes from local bending to global bending (see Fig. 5). Equations (13) and (14) answer exactly for global bending. Hence, for the prediction of the Young's modulus of carbon nanotubes by bending methods, we have to consider nanotubes with aspect ratios of up to 8 to obtain more exact results.

4 Young's modulus of defective SWCNTs

4.1 Vacancy defects

Due to the restrictions of CNT manufacturing, the production of perfect nanotubes is very hard, and the percentage of those is very low compared to the percentage of defective nanotubes. Vacancies result from missing carbon atoms in the CNT walls. This can happen when CNTs are subjected to irradiation. The types of vacancy defects for the study of defects in carbon nanotubes are illustrated in Fig. 7. Vacancies result from missing carbon atoms in the CNT walls. The defects included are single vacancies (one atom missing), double vacancies (two adjacent atoms missing) and triple vacancies (three adjacent atoms missing). By removing the

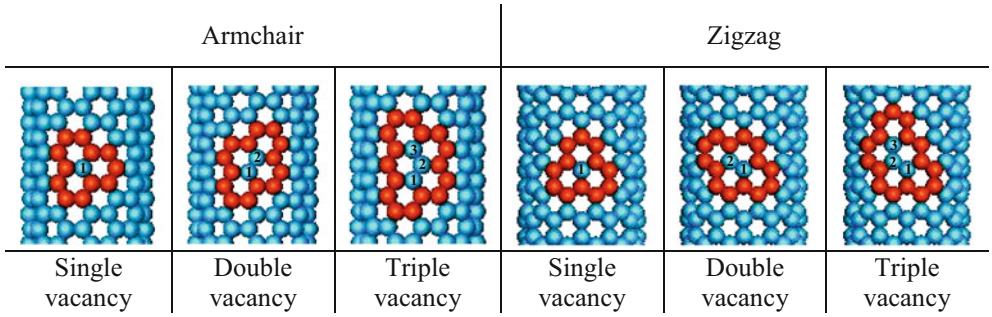

Fig. 7 Different vacancy defects used in the analysis (removed carbon atoms indicated by numbers)

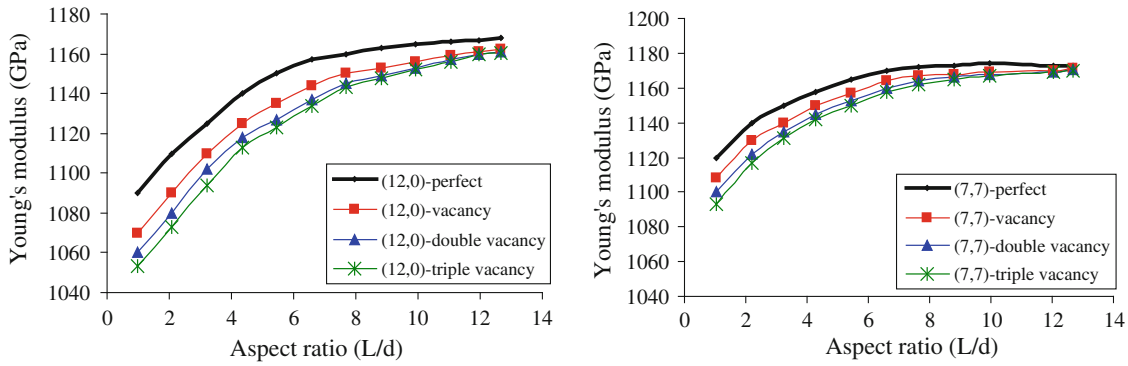

Fig. 8 Influence of vacancy defects on the Young's modulus with variation of the nanotube length by the tension test

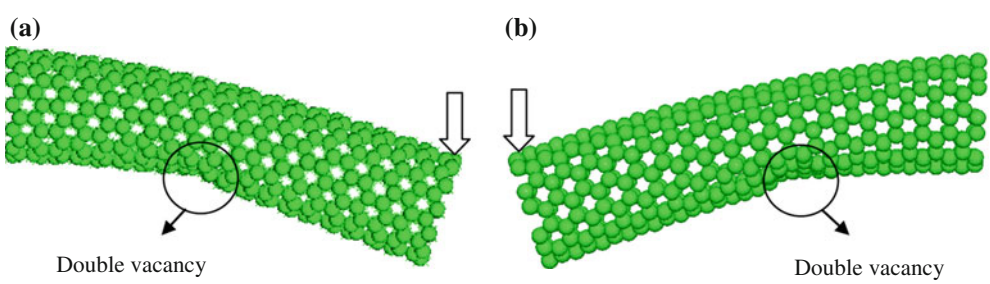

Fig. 9 Deformed configuration of defective zigzag (12, 0) (**a**) and armchair (7, 7) (**b**) nanotubes with one double vacancy subjected to free-fixed bending

carbons atoms from the nanotube, all of the interactions (springs and connectors) between bonds will remove. All of the defects are situated in the middle of the nanotube.

For zigzag (12, 0) and armchair (7, 7) nanotubes with vacancy defects under tension, the Young's modulus as a function of the nanotube length is shown in Fig. 8. It is seen that the influence of vacancy defects on the Young's modulus for both zigzag and armchair nanotubes decreases with increasing nanotube length, and these defects have more effect on the Young's modulus at short lengths. Furthermore, zigzag nanotubes are more sensitive to variations of the length at short lengths. The main reason for this is the different orientation of the vacancy defects (see Fig. 7). Another reason for this difference is due to the orientation of the C-C bonds for zigzag CNTs that are in the load direction. Therefore, the distribution of load on the carbon atoms for zigzag and armchair CNTs is uniform in the circumferential and axial direction, respectively.

Figure 9 shows the deformed configuration of the nanotube with vacancy defects after free-fixed bending tests for zigzag and armchair nanotubes. As observed in Fig. 9, vacancy defects cause a nick at the defect location.

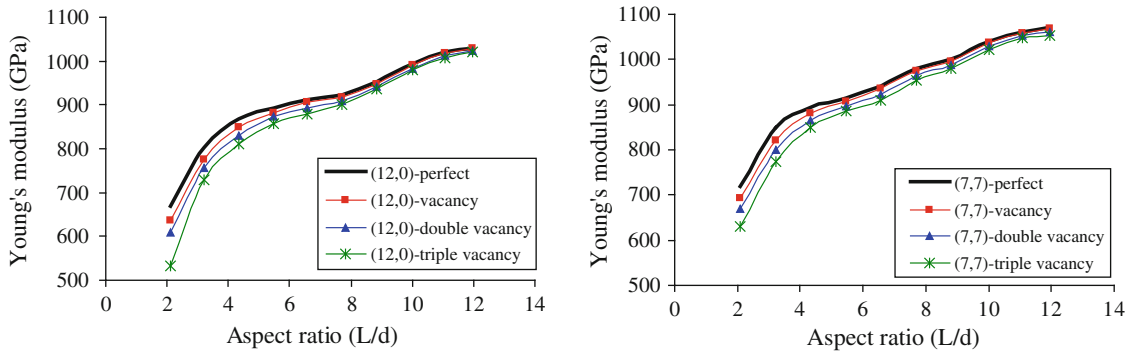

Fig. 10 Influence of vacancy defects on the Young's modulus with variation of the nanotube length by the free-fixed test

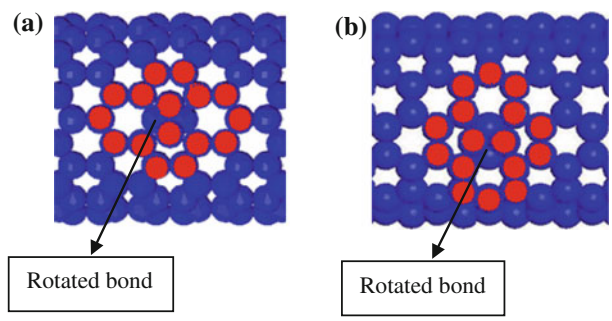

Fig. 11 Configuration of Stone-Wales defects in zigzag (**a**) and armchair (**b**) nanotubes (indicated by *solid spheres*)

In Fig. 10, the comparison of the Young's modulus of perfect and defective SWCNTs with vacancy defects by the free-fixed bending test is illustrated. It can be observed that, for the same length and diameter, the Young's modulus of the armchair nanotube is higher than that of the zigzag nanotube. Furthermore, it can be seen that values of the Young's modulus are more sensitive to vacancy defects for shorter tubes. With increasing nanotube length, the influence of vacancy defects decreases.

4.2 Stone-Wales defects

Defects are generated in the synthesizing process and they can also be caused by mechanical manipulation. The most typical structural defects are Stone-Wales defects [30]. Stone-Wales defects in carbon nanotubes are generated under certain conditions. These topological defects are regions in a crystal where the normal chemical-bonding environment is topologically different from the surroundings. The carbon nanotubes contain regions where the number of atoms in a ring is different from six, while the total number of atoms remains the same. Stone and Wales showed that a dipole consisting of a pair of 5–7 rings can be created by rotating the C-C bond in a hexagonal network by 90°. As shown in Fig. 11, in this rotation, four hexagons are changed into two heptagons and two pentagons.

Here, we suppose that an initial Stone-Wales defect exists on the nanotube before the tension test (see Fig. 11). Unlike the vacancy defects in which bonds have been removed, the carbon bonds in Stone-wales defects will not remove but will rotate. This defect is in the middle of the nanotube.

Table 1 summarizes the Young's moduli obtained from perfect nanotubes and compares them with those of nanotubes with Stone-Wales defects. The Young's modulus is found for nanotubes with Stone-Wales defects with different diameters and lengths by the tension and free-fixed bending tests. Generally, the effect of Stone-Wales defects on the decrease of the Young's modulus is much lower than vacancy defects, and these weak defects do not have a significant effect on the Young's modulus of the nanotubes. The main reason for this are the removed bonds of the vacancy defects. In addition, with increasing nanotube length and diameter, the influence of Stone-Wales defects decreases.

Table 1 The variation of Young's modulus of a carbon nanotube with model size, type of method and Stone-Wales defects

Tube size (nm)		Young's modulus (TPa)			
		Tension		Free-Fixed bending	
Chirality	Length	No defect	Stone-wales	No defect	Stone-wales
(12, 0)	4.118	1,140	1,132	869	860
(12, 0)	12.354	1,167	1,165	1,030	1,029
(7, 7)	4.058	1,158	1,155	895	891
(7, 7)	12.174	1,173	1,172	1,072	1,072
(16, 0)	4.118	1,148	1,144	875	870
(16, 0)	12.354	1,169	1,168	1,033	1,032
(9, 9)	4.058	1,165	1,163	902	898
(9, 9)	12.174	1,174	1,174	1,075	1,073
(22, 0)	4.118	1,150	1,149	879	878
(22, 0)	12.354	1,170	1,170	1,034	1,034
(13, 13)	4.058	1,166	1,166	903	901
(13, 13)	12.174	1,175	1,175	1,077	1,077

5 Conclusion

Various methods for the prediction of the Young's modulus of SWCNTs have been investigated via the structural mechanics model. For all of the experimental tests that were used for the prediction of the Young's modulus, we needed to select a sufficiently long nanotube. This option is more sensitive for fixed–fixed and simple–simple bending tests. The best method for the prediction of the Young's modulus of single-walled carbon nanotubes is the tension test. Defects do not have a significant effect on the Young's modulus of sufficiently long SWCNTs. However, for nanotubes with shorter lengths, this effect is much more significant, and armchair nanotubes are more sensitive to defects than zigzag nanotubes in general.

References

1. Iijima, S.: Helical microtubules of graphitics carbon. Nature **354**, 56–58 (1991)
2. Nardelli, M.B., Fattebert, J.L., Orlikowski, D., Roland, C., Zhao, Q., Bernholc, J.: Mechanical properties, defects and electronic behavior of carbon nanotubes. Carbon **38**, 1703–1711 (2003)
3. Iijima, S., Ichlhashi, T.: Single-shell carbon nanotubes of 1-nm diameter. Nature **363**, 603–605 (1993)
4. Wong, E.W., Sheehan, P.E., Lieber, C.M.: Nanobeam mechanics: elasticity, strength, and toughness of nanorods and nanotubes. Science **277**, 1971–1975 (1997)
5. Krishnan, A., Dujardin, E., Ebbesen, T.W., Yianilos, P.N., Treacy, M.M.J.: Young's modulus of single-walled nanotubes. Phys. Rev. B **58**, 14013–14019 (1998)
6. Salvetat, J., Bonard, J., Thomson, N.H., Kulik, A.J., Forro, L., Benoit, W., Zuppiroli, L.: Mechanical properties of carbon nanotubes. Appl. Phys. A **69**, 255–260 (1999)
7. Tombler, T.W., Zhou, C., Alexseyev, L., Kong, J., Dai, H., Liu, L., Jayanthi, C.S., Tang, M., Wu, S.: Reversible electromechanical characteristics of carbon nanotbues under local-probe manipulation. Nature **405**, 769–772 (2000)
8. Yu, M., Files, B., Arepalli, S., Ruoff, R.: Tensile loading of ropes of single wall carbon nanotubes and their mechanical properties. Phys. Rev. Lett. **84**, 5552–5555 (2000)
9. Li, C.Y., Chou, T.S.: A structural mechanics approach for the analysis of carbon nanotubes. Int. J. Solids Struct. **40**, 2487–2499 (2003)
10. Tserpes, K.I., Papanikos, P.: Finite element modeling of single-walled carbon nanotubes. Compos. Part B. **36**, 468–477 (2005)
11. Hu, N., Fukunaga, H., Lu, C., Kameyama, M., Yan, B.: Prediction of elastic properties of carbon nanotube-reinforced composites. Series A. Math. Phys. Sci. **461**, 1685–1710 (2005)
12. Kalamkarov, A.L., Georgiades, A.V., Rokkam, S.K., Veedu, V.P., Ghasemi-Nejhad, M.N.: Analytical and numerical techniques to predict carbon nanotubes properties. Int. J. Solids Struct. **43**, 6832–6854 (2006)
13. Meo, M., Rossi, M.: Tensile failure prediction of single wall carbon nanotube. Eng. Fract. Mech. **73**, 2589–2599 (2006)
14. Natsuki, T., Tantrakarn, K., Endo, M.: Prediction of elastic properties of single-walled carbon nanotubes. Carbon **42**, 39–45 (2003)
15. Odegard, G.M., Gates, T.S., Nicholson, L.M., Wise, K.E.: Equivalent-continuum modeling with application to carbon nanotubes. NASA/TM, 211454 (2002)
16. Yakobson, B.I., Brabec, C.J., Bernholc, J.: Nanomechanics of carbon tubes: instability beyond linear response. Phys. Rev. Lett. **76**, 2511–2514 (1996)
17. Cornwell, C.F., Wille, L.T.: Elastic properties of single-walled carbon nanotubes in compression. Solid State Commun. **101**, 555–558 (1997)
18. Lu, J.P.: Elastic properties of carbon nanotubes and nanoropes. Phys. Rev. Lett. **79**, 1297–1300 (1998)
19. Yao, N., Lordi, V.: Young's modulus of single-walled carbon nanotubes. J. Appl. Phys. **84**, 1939–1943 (1998)

20. Goze, C., Vaccarini, L., Henrard, L., Bernier, P., Hernandez, E., Rubio, A.: Elastic and mechanical properties of carbon nanotubes. Synth. Metals. **103**, 2500–2501 (1999)
21. Lier, G.V., Alsenoy, C.V., Doren, V.V., Geerlings, P.: Ab initio study of the elastic properties of single-walled carbon nanotubes and grapheme. Chem. Phys. Lett. **326**, 181–185 (2000)
22. Kudin, K.N., Scuseria, G.E., Yakobson, B.I.: 2F, BN and C nanoshell elasticity from ab initio computations. Phys. Rev. B. **64**, 235406 (2001)
23. Belytschko, T., Xiao, S.P., Schatz, G.C., Ruoff, R.S.: Atomistic simulations of nanotube fracture. Phys. Rev. B. **65**, 235–430 (2002)
24. Troya, D., Mielke, S.L., Schatz, G.C.: Carbon nanotube fracture—differences between quantum mechanical mechanisms and those of empirical potentials. Chem. Phys. Lett. **382**, 133–141 (2003)
25. Shen, L., Li, J.: Transversely isotropic elastic properties of single-walled carbon nanotubes. Phys. Rev. B. **69**, 045414 (2004)
26. Xiao, J.R., Gama, B.A., Gillespie, J.W.: An analytical molecular structural mechanics model for the mechanical properties of carbon nanotubes. Int. J. Solids Struct. **42**, 3075–3092 (2005)
27. Huang, Y., Wu, J., Hwang, K.C.: Thickness of graphene and single-wall carbon nanotubes. Phys. Rev. B. **74**, 245413–245419 (2006)
28. Parvaneh, V., Shariati, M., Majd Sabeti, A.M.: Investigation of defects effects on the buckling behavior of SWCNTs via a structural mechanics approach. Eur. J. Mech. A/Solids **28**, 1072–1078 (2009)
29. Rappe, A.K., Casewit, C.J., Colwell, K.S. et al.: UFF, A full periodic-table force-field for molecular mechanics and molecular dynamics simulations. J. Am. Chem. Soc. **114**, 10024–10035 (1992)
30. Stone, A.J., Wales, D.J.: Theoretical studies of icosahedral C60 and some related species. Chem. Phys. Lett. **128**, 501–503 (1986)